Total cross sections for collisions of H^- and D^- with various molecules

M. S. Huq, L. D. Doverspike, and R. L. Champion
Department of Physics, College of William and Mary, Williamsburg, Virginia 23185
(Received 24 May 1982)

Absolute cross sections for electron detachment and charge transfer (or dissociative charge transfer) have been measured for collisions of H^- and D^- ions with N_2, CO, O_2, CO_2, and CH_4. The relative collision energies investigated range from a few eV up to several hundred eV. Electron detachment is found to be the dominant process for all the molecular targets except O_2 for which charge transfer dominates. Isotope effects are observed in all the cross sections. Isotopic substitution reveals that the detachment cross sections scale with relative collision energy at low collision energies and with relative collision velocity at high collision energies. The general features of the charge-transfer cross section for the O_2 target are in agreement with the ideas of a simple two-state collision model. The cross sections for charge transfer (or dissociative charge transfer) are found to be small for all targets except O_2.

I. INTRODUCTION

Recent studies of the collisional detachment of atomic negative ions by molecular targets have revealed that electron detachment is an important product channel in such collisions and may proceed by any of several distinct mechanisms. The most common detachment mechanism is perhaps direct detachment in which the loosely bound electron of the negative ion is promoted into the continuum by either a curve (surface) crossing mechanism or a coupling of the nuclear motion of the collision partners to the electronic motion. For atomic targets, examples of these two processes have been studied experimentally and described theoretically for the systems $H^- + He$ and $H^- + Ne$.[1,2]

In addition to direct detachment, several other processes have been found to be important for electron detachment in collisions of negative ions with molecular targets. One such mechanism involves an initial charge transfer to a shape resonance of the molecular target followed by a rapid decay of the negative molecular ion,

$$X^- + BC \rightarrow (BC^-)^* + X \rightarrow BC^* + e + X \ , \qquad (1)$$

which likely leaves the target molecule excited. Evidence for this type of process has been found in the kinetic energy spectra of the detached electrons[3] as well as in the time-of-flight spectra for the fast neutral products of collisional detachment.[4,5]

Another mechanism of electron detachment by molecular targets is one in which reactive scattering accompanies detachment,[6] as in

$$X^- + BC \rightarrow XB + C + e \ . \qquad (2)$$

Finally, at the lowest collision energies, there is always the possibility of associative detachment[7] for selected reactants as in

$$X^- + BC \rightarrow XBC + e \ . \qquad (3)$$

In general, the relative importance of (2) and (3) increases as the collision energy is lowered. Associative detachment is only important at low relative collision energies, $E \lesssim 1$ eV, and reactive scattering [i.e., (2)] is important for $E \lesssim 10$ eV. For higher collision energies, i.e., $E \lesssim 1000$ eV, both direct detachment and detachment via charge transfer have been observed to be of similar magnitude for the few systems studied thus far.[5] For example, the time-of-flight studies of the collisional detachment of H^- by N_2 by Tuan and Esaulov indicate that the total cross sections for direct detachment and detachment via charge transfer are approximately equal at $E \simeq 500$ eV.[5] Theoretical calculations for (1) have been made by Gauyacq and Herzenberg for selected systems by using electron-molecule scattering data [analogous to the reverse of (1)] to compute the total cross sections and time-of-flight spectra expected for (1).[8] These studies have been limited to collision energies in the keV range.

The purpose of this paper is to present the results of measurements of absolute electon detachment cross sections for collisions of H^- and D^- ions with N_2, CO, O_2, CO_2, and CH_4. The energy range of the experiments is from about 1 eV up to several hundred eV. The collisional detachment of both H^- and D^- has been studied in order to determine the effects of isotopic substitution upon the total de-

tachment cross sections. Such "isotope effects" may provide valuable insights as to which mechanisms are responsible for detachment and these effects are often instrumental to a complete understanding of the collisional dynamics.

In addition to the results of the total cross sections for electron detachment, we also report measurements for the production of "slow" negative ions for collisions of the reactants listed above. Processes which give rise to these slow negative ions include charge transfer,

$$H^- + O_2 \rightarrow O_2^- + H \ , \tag{4}$$

and dissociative charge transfer as in

$$H^- + CO_2 \rightarrow H + CO + O^- \ . \tag{5}$$

In several cases it is possible to see how such mechanisms compete with electron detachment.

In what follows, we will discuss the experimental method and then present the results for each molecular target separately.

II. EXPERIMENTAL PROCEDURE

The apparatus used in these experiments has been described in detail elsewhere.[6,9,10] Briefly, H^- or D^- ions, produced in an arc-discharge-type ion source, are extracted and electrostatically focused into a Wien velocity filter which serves as a mass spectrometer. The ion beam then enters the collision region which is shown schematically in Fig. 1. The laboratory kinetic energy of the primary ion beam is

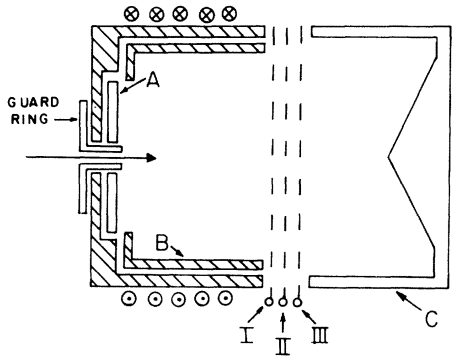

FIG. 1. A schematic diagram of the collision chamber used for total-cross-section measurements is given. An axial magnetic field along with an electrostatic field between grids I and II traps the detached electrons to plate *A*. Current at *B*, which is due primarily to low-energy heavy particles (viz., O^-, O_2^-, etc.) can be monitored separately. The primary beam, which enters from left on the figure, can be monitored by the element *C*. The size of the guard ring is exaggerated. It comprises about 4% of the area of plate *A*.

determined by electrostatic retardation within the collision chamber and is accurate to within a quarter of an eV. The full width at half maximum for both H^- and D^- ion beams typically varies from about 0.2 eV at the lowest collision energies up to a maximum of about 0.6 eV above collision energies of 50 eV.

The target gas is maintained at room temperature and the target gas pressure in the collision region is usually in the range of 10^{-4} torr during the experiments. The background pressure prior to admitting the scattering gas into the collision chamber is typically 10^{-7} torr. The absolute pressure within the collision chamber is determined with a capacitance manometer and the target gas may be quickly cycled into and out of the collision chamber to monitor background signals in the cross-section measurements. The capacitance manometer is connected directly to the collision chamber by a $\frac{1}{4}$-in. tube, approximately 5 in. in length.

There are several distinct processes that may result from collisions of negative ions with molecules. The processes that are important in the present studies are

$$H^- + BC \rightarrow e + \text{products} \ , \tag{6}$$

$$H^- + BC \rightarrow (BC)^- + H \ , \tag{7}$$

$$H^- + BC \rightarrow B^- + HC \ , \tag{8}$$

$$H^- + BC \rightarrow H^- + BC \ , \tag{9}$$

$$H^- + BC \rightarrow H^- + (BC)^* \ , \tag{10}$$

$$H^- + BC \rightarrow B^- + H + C \ . \tag{11}$$

Equation (6) corresponds to the production of free electrons by any collisional detachment mechanism. The collision chamber provides a trap for these detached electrons in the following manner. An axial magnetic field is maintained within the collision chamber with a magnitude (5—10 G) so that the cyclotron radii of the detached electrons is less than the radius of element *A* (see Fig. 1). Detached electrons with upstream longitudinal momenta go directly to element *A*. A weak electric field between grids I and II reflects the remaining electrons with opposite longitudinal momenta to plate *A*. In order to ensure that all electrons are reflected to element *A*, it is sufficient that the electrostatic potential between grids I and II be about 8% of the laboratory kinetic energy of the primary ion beam with a maximum of 5 V. To assure that a negligible fraction of the detached electrons is collected on the guard ring which projects into the collision region (see Fig. 1) the guard ring is maintained at a slightly negative bias of about 0.2 V. Such a bias voltage saturates the electron current to element *A*. For the systems being

investigated there are several ways in which, not only electrons, but negatively charged ions as well, reach element A. This causes some ambiguity about the nature of the signal observed on A. For the light-on-heavy systems reported in this study, laboratory backscattering of elastically or inelastically scattered primary ions [Eqs. (9) and (10)] is possible. Such events are most probable only at very low collision energies and can "contaminate" the measurements of electron detachment cross sections for energies under a few eV. A detailed discussion about the magnitude of this effect has been given previously.[9] A second and not necessarily insignificant contribution to the ion signal observed on element A will be due to "slow" ions which arise from charge transfer or ion-molecule reactions as in (7), (8), or (11). Let us denote the cross section for forming slow product ions as $\sigma_I(E)$, where this is the true cross section for (7), (8), and (11). If we assume that $d\sigma_I/d\Omega$ has an angular distribution which is isotropic, then 20% of all product ions will arrive at element A and 80% will be detected on element B. This figure (20%) results from averaging (along the collision path) the solid angle subtended by element A for both forward- and backward-moving product ions. Specular reflection by the trapping electric field is assumed for the ions which are initially moving in the forward (primary ion beam) direction. If $d\sigma_I/d\Omega$ is zero for laboratory scattering angles, $\theta \gtrsim 90°$ (no backscattered products) and isotropic in the forward hemisphere, then only 2.3% of the slow ions arrive at A.

In summary, the measurements of the electron detachment cross sections, $\sigma_e(E)$, which are based on the signal observed at element A may overestimate the true detachment cross section by as much as 20% of $\sigma_I(E)$. For all of the targets except O_2, this is inconsequential since $\sigma_e(E)/\sigma_I(E) \sim 5-10$. The measurements of $\sigma_e(E)$ are reproducible to within 5%. Systematic errors (e.g., pressure and path length measurements) when combined with the uncertain contamination from slow product ions limit the accuracy of the detachment cross section to an uncertainty of $\sim 15\%$ except for the O_2 target where the uncertainty is 20%. Both H^- and D^- are in the ion beam and the measurements for each isotope are made by allowing the appropriate ion to pass through the Wien filter. The ratios of the cross sections, $\sigma_e(E,H^-)/\sigma_e(E,D^-)$, are accurate to 2%.

The slow negative ions that result from charge transfer, ion-molecule reaction, or dissociative charge transfer [i.e., Eqs. (7), (8), and (11)] will be collected primarily on element B. The electrostatic potential that has been used to trap the detached electrons is also used to confine these slow ions to the left of grid II (see Fig. 1). An additional contribution to the signal observed on B may arise from large angle ($\theta \gtrsim 40°$) elastic or inelastic scattering of the primary negative ions. The present apparatus does not have any provision for mass analyzing the product ions and hence cannot distinguish between the slow product ions and elastically or inelastically scattered primary ions. Thus the signal on B cannot be unambiguously identified.

For higher collision energies, the partial cross sections due to large-angle scattering of the primary negative ions should be small and this has been found to be the case for rare-gas targets. For example, in the case of collisions of H^- and D^- with Ne, the signal observed on B drops smoothly with a resultant partial (large-angle) cross section of about $0.5\,a_0^2$ at $E = 150$ eV.

In summary, cross-section measurements based upon products which arrive at element B give an approximate indication of $\sigma_I(E)$, as defined earlier. The principal reasons for a lack of precision in the measurement of $\sigma_I(E)$ are (i) some slow product ions will arrive at A rather than B (20% for isotropic distribution), and (ii) the partial cross section for large-angle scattering of H^- (or D^-), which may be as high as a few a_0^2, contributes to the signal on element B. This latter process tends to cause an overestimation of $\sigma_I(E)$ whereas the former causes an underestimation of $\sigma_I(E)$. As for the aforementioned measurements of $\sigma_e(E)$, these effects vary for each target and they will be discussed separately.

III. RESULTS AND DISCUSSION

A. $H^-(D^-)+N_2$

The experimental results for the total electron detachment cross section $\sigma_e(E)$ for collisions of $H^-(D^-)$ with N_2 are given in Fig. 2 as a function of relative collision energy (i.e., the energy in the center-of-mass reference frame). Detachment cross sections for these systems over the energy range 2—100 eV were reported previously.[11] The high-energy measurements of these previous experiments did not appear to extrapolate smoothly to the measurements of Risley and Geballe.[12] It was suggested that this "connection" problem might be due to sudden increases in the cross sections in the energy range not covered by either experiment. Thus it was felt that total electron detachment cross sections for these systems should be remeasured with special emphasis on the energy region not covered by any experiments. The present experiments have also been extended to lower collision energies than the previous measurements.

The present results for $\sigma_e(E)$ are about 10% below earlier measurements,[11] except in the near-

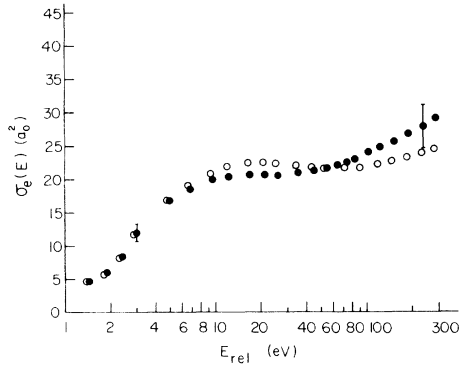

FIG. 2. Total electron detachment cross sections σ_e for H^- and D^- on N_2 are given as a function of relative collision energy. The filled circles are the results for H^- projectiles and the open circles are the results for D^-. The dotted line is a representative of the results of Risley and Geballe.[12] Error bars on this and subsequent figures represent our estimate of the systematic uncertainty in the measurements—any systematic error should be independent of which isotope is being studied.

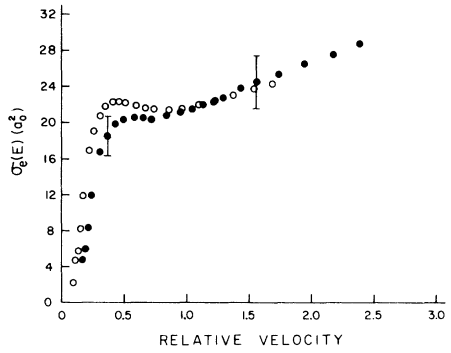

FIG. 3. Total electron detachment cross sections σ_e for H^- and D^- on N_2 are given as a function of relative collision velocity, which is expressed in units of 10^7 cm/sec. The filled circles are the results for the H^- projectiles and the open circles are for D^-.

threshold region ($E \lesssim 6$ eV) where the present measurements lie about 20% lower. The 10% discrepancy has been noted before[9] and was attributed to possible errors in determining the target gas pressure in the previous measurements. The larger error in the near-threshold region is a consequence of using a primary ion beam in the present experiments which has a much narrower energy width than that used in previous experiments, since any broadening effect tends to increase the apparent cross section in the near-threshold region. The measured low-energy cross sections for $\sigma_e(E)$ should not be contaminated by any low-energy product ions, since $\sigma_I(E)=0$ for the $H^-(D^-)+N_2$ systems.

An important feature of the cross sections shown in Fig. 2 is the observation of a dual isotope effect when σ_e is exhibited as a function of E: at the higher relative collision energies, the reactants with the higher relative collision velocity exhibit the larger detachment cross section whereas the trend is just the opposite at low relative collision energies. It is possible that this difference is due to the fact that there are different mechanisms which dominate the detachment in the high- and low-energy regions. The magnitude of the low-energy isotope effect varies from about 5—10% over the energy range 10—40 eV and is consistent with a description of electron detachment that involves the crossing or merging of the discrete reactant state (which represents the interaction potential of the negative ion with N_2) with the continuum of product states (representing $H+N_2$ along with a free electron of arbitrary energy). According to this description, for a given E, both D^- and H^- will follow the same trajectories but with different velocities (the isotopic masses being different) and hence the time spent by D^- in the continuum is larger than that of H^-, resulting in a larger detachment cross section for D^-.

At higher relative collision energies (i.e., $E > 50$ eV), the isotope effect reverses its character, where the faster reactants give the larger detachment cross section. In addition, it is found that the detachment cross sections in this energy region (i.e., $E > 50$ eV), increase with relative collision energy and more importantly scale with relative collision velocity; for the same relative collision velocity the cross sections for the isotopic doublet are approximately the same. This can be seen very clearly from Fig. 3 where the electron detachment cross sections for both isotopes are plotted as a function of relative collision velocity. The experimental results for these systems illustrate that the detachment cross sections are not the same function of relative collision energy, nor are they the same functions of relative collision velocity over the energy range 1—200 eV. The present experiments thus connect two regions: at low collision energy, detachment cross sections for both isotopes are found to be the same at identical collision energies, whereas at high collision energy, detachment cross sections are found to scale with relative collision velocity. For collision energies greater than several hundred eV, this velocity scaling for $H^-(D^-)+N_2$ has been investigated previously[12] and has been found to be valid for energies up to at least 10 keV.

It was mentioned in the Introduction that an important contribution to detachment may arise from a process which involves an initial charge transfer to a shape resonance of the molecular target, followed very quickly by decay of the molecular negative ion. This charge transfer process has been studied by Tuan and Esaulov[5] for $200 \lesssim E \lesssim 1000$ eV and is

found to be quite important in the collisional detachment of H^- by N_2. The energy-loss spectra of the scattered H atoms show three distinct peaks which the authors attribute to direct detachment, detachment via charge transfer and detachment with electronic excitation of N_2. They estimate that 25% of the total electron detachment cross section at $E \simeq 500$ eV is due to detachment with excitation and the remainder is distributed equally between direct detachment and detachment via charge transfer to a shape resonance of N_2^-. It is reasonable to suggest that the increase in $\sigma_e(E)$, for $E \gtrsim 50$ eV is due to the onset of detachment via charge transfer. Despite this increase in $\sigma_e(E)$, the present results still fall about 30% below a previous measurement[12] for electron detachment in $H^- + N_2$ collisions at 193 eV.

The cross sections obtained from the signal observed on element B, which we will denote as $\sigma_B(E)$, for collisions of $H^-(D^-)$ with N_2 are shown in Fig. 4 as a function of relative collision energy. Also shown in the figure are measurements of $\sigma_B(E)$ for collisions of both H^- and D^- with Ne.

Since $\sigma_I(E)$ should be zero for these reactants, we can view $\sigma_B(E)$ as presented in Fig. 4 as the partial (large-angle) elastic and inelastic scattering cross section. The results for Ne represent a partial cross section for only elastic scattering, whereas the minima observed at 9.5 eV for the N_2 target no doubt indicates the region where the partial inelastic and elastic cross sections are comparable.

For a given E and impact parameter b, the c.m. scattering angle (suitably averaged over molecular orientations) for H^- should be equal to that for D^- for potential scattering. However, the laboratory scattering angle for H^- will be slightly greater. This may be the reason that $\sigma_B(E,H^-)/\sigma_B(E,D^-) > 1$, but such effects cannot be separated from possible velocity-dependent collision mechanisms which may be operative.

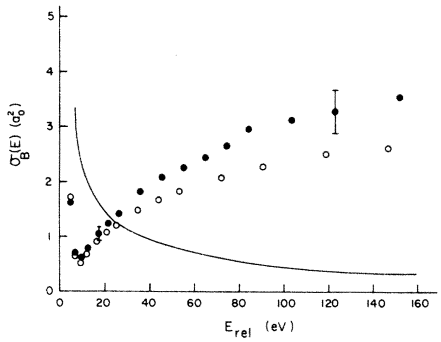

FIG. 4. Total cross sections for partial elastic and inelastic scattering, σ_B, as described in the text are given for the $H^-(D^-)+N_2$ system as a function of relative collision energy. The filled circles are the results for H^- and the open circles are for D^-. Also given in the figure is a curve representative of the partial cross section for large-angle elastic scattering of H^- and D^- by Ne.

B. $H^-(D^-)+CO$

Figure 5 shows the measured electron detachment cross sections $\sigma_e(E)$ for collisions of H^- and D^- with CO as a function of relative collision energy. A comparison of the detachment cross sections for the CO target with those for N_2 shows that $\sigma_e(E)$ for CO is similar in shape and magnitude to the results for N_2, especially in the high-energy range. Furthermore, for $E \gtrsim 50$ eV, $\sigma_e(E)$ for CO scales approximately with relative collision velocity. At low collision energies (i.e., $E < 30$ eV), the detachment cross sections are found to scale with relative collision energy, with no discernible isotope effect. The scaling behavior suggests that electron detachment proceeds via two distinct mechanisms, one dominating at energies below ~ 30 eV and a different process showing up at higher energies.

The importance of charge exchange in $H^- + CO$ collisions has been investigated by Tuan and Esaulov.[5] Their measurements on the energy-loss spectra of neutral H atoms produced in collisions of 420-eV H^- with CO indicate that the contribution of the $^2\Pi$ resonance of CO to electron production is comparable to that from direct detachment. The increase in $\sigma_e(E)$ with energy, for $E > 50$ eV, may then be due to detachment via charge transfer to a shape resonance of $CO^-(^2\Pi)$. For $E < 50$ eV, $\sigma_e(E)$ can be described by the crossing or merging of the negative-ion bound state with the continuum of states representing a neutral molecule and a free electron of arbitrary energy.

As in N_2, a small signal is observed for CO on element B. The cross sections $\sigma_B(E)$ for CO are shown in Fig. 6 as a function of relative collision energy.

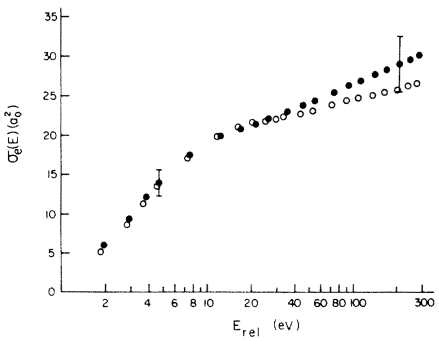

FIG. 5. Absolute total cross sections for electron detachment, σ_e, for collisions of H^- and D^- wtih CO are given as a function of relative collision energy. The filled circles are the results for H^- and the open circles are for D^-.

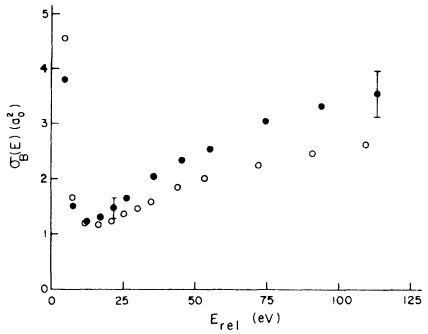

FIG. 6. $\sigma_B(E)$, as discussed in the text, is given for collisions of H^- and D^- with CO as a function of relative collision energy. The filled circles are the results for H^- and the open circles are for D^-.

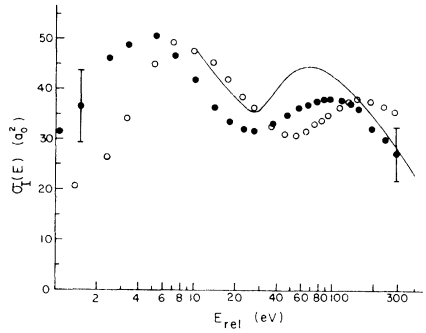

FIG. 7. The total charge-transfer cross sections for H^- and D^- on O_2 are given as a function of relative collision energy. The filled circles are the present results for H^- and the open circles are for D^-. The solid line is a curve representative of the results of Bailey and Mahadevan for slow-ion production for collisions of H^- with O_2.

These results are essentially identical to those for N_2 with the same isotope effect. Based upon this similarity to N_2 (where $\sigma_I=0$) it is reasonable to assume that σ_I is quite small for CO. Consequently there should be a negligible flux of product ions resulting from the reactions

$$H^- + CO \rightarrow O^- + \text{products}$$
$$\rightarrow C^- + \text{products},$$

and the results presented in Fig. 5 for $\sigma_e(E)$ will not be contaminated by such ions.

The minima in $\sigma_B(E)$ for both isotopes occur at about 12 eV (compared to 9.5 eV for N_2). The increasing signal observed for $E<12$ eV is due to large-angle elastic scattering of the primary ions. For $E>12$ eV, the signal is probably due to large-angle inelastic scattering of the primary negative ions.

C. $H^-(D^-)+O_2$

For these reactants, there are several different product channels that are important in the present studies. For the H^- projectile, they include

$$H^- + O_2 \rightarrow H + O_2 + e \quad (0.75 \text{ eV}), \tag{12}$$
$$\rightarrow HO_2 + e \quad (\lesssim -1 \text{ eV}), \tag{13}$$
$$\rightarrow O_2^- + H \quad (0.31 \text{ eV}), \tag{14}$$
$$\rightarrow OH^- + O \quad (-0.36 \text{ eV}), \tag{15}$$
$$\rightarrow O^- + OH \quad (0.003 \text{ eV}), \tag{16}$$
$$\rightarrow O^- + O + H \quad (4.403 \text{ eV}). \tag{17}$$

The energy defects for ground-state reactants and products are also given along with each channel. The measurements of the cross sections for electron detachment, $\sigma_e(E)$, for these systems are influenced somewhat by channels (14)–(17), i.e., the production of slow negative ions. Thus, the measurements of the cross sections for slow-ion production, $\sigma_I(E)$, will be discussed first [by assuming $\sigma_I(E)\simeq\sigma_B(E)$], followed by a discussion of electron detachment.

The experimental results for $\sigma_I(E)$ for collisions of both H^- and D^- with O_2 are given in Fig. 7 where the cross sections are presented as a function of the relative collision energy. Also given in the figure is a curve representative of the results of Bailey and Mahadevan[13] for the production of slow ions in collisions of H^- with O_2. As is clear in the figure, the cross sections exhibit two distinct peaks for both isotopes in two different regions of energy. In order to identify the products contributing to $\sigma_I(E)$, experiments were done for the $D^- + O_2$ system on an apparatus used for differential cross-section measurements. This differential apparatus employs a quadrupole mass spectrometer to determine the mass of the product ions and has been described in detail previously.[14] The energy range for these experiments was from about 5 eV up to 150 eV. An extensive search for low-energy O_2^-, OD^-, and O^- was carried out, revealing that at least 98% of the slow product ions were O_2^-. Hence, the measurements presented in Fig. 7 are for the production of O_2^-, as given by Eq. (14). The O_2^- thus produced will have vibrational quantum numbers $v' \lesssim 3$, since the energy of the O_2^- $(v'=3)$ molecular ions lies slightly below that of O_2 $(v=0)$. For $v'>3$, $O_2^-(v')$ is unstable with respect to electron detachment.

A striking feature of the cross sections shown in Fig. 7 is the strong isotope effect observed over the entire energy range. The most remarkable feature of $\sigma_I(E)$ is seen when the cross sections due to different isotopes are compared at identical collision velocities rather than identical relative energies. Such plots are shown in Fig. 8 where the cross sections $\sigma_I(E)$ are displayed as a function of relative

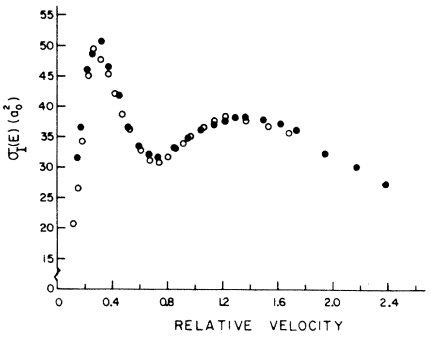

FIG. 8. The total charge-transfer cross sections for H^- and D^- on O_2 are given as a function of relative collision velocity, which is expressed in units of 10^7 cm/sec. The filled circles are for H^- and the open circles are for D^-.

collision velocity. As can be seen from the figure, the cross sections for each isotope are the same at the same relative collision velocity.

In an attempt to understand the mechanism(s) responsible for such a behavior, let us assume that the basic dynamics for the charge transfer can be described within the framework of a two-state problem in which the initial and final states involved in the process are given by

$$H^- + O_2\ (v=0) \rightarrow H + O_2^-\ (v'=3)\ .$$

The asymptotic energy difference (ΔE) between these two states is given approximately by the electron affinity of the hydrogen atom (0.75 eV). In a two-state approximation, the total cross section contains an oscillatory term which depends upon the collision velocity,[15]

$$\sigma(v) \sim M(v) \sin^2\left[\frac{\Delta E z}{2v}\right]\ . \tag{18}$$

In Eq. (18), z/v represents the average time spent in the region where transitions can take place and $M(v)$ represents the coupling of the initial state ($H^- + O_2$) to the final state ($H + O_2^-$).

It is interesting to note that, by inserting reasonable values of z and ΔE into Eq. (18), the two maxima and one minimum of Fig. 8 are well reproduced, as is indicated in Table I. Moreover, the total cross section which should be on the order of $\pi(z/2)^2$ is observed to be just this value. The isotope effect which is observed is compatible with this rather simple model.

TABLE I. A comparison of the observed extrema of Fig. 8 and those predicted by Eq. (18) with $\Delta E = 0.75$ eV and $z = 7a_0$.

Velocities at which extrema are observed (10^6 cm/sec)	Velocities at which extrema are predicted from Eq. (18) (10^6 cm/sec)	$\frac{\Delta E z}{v}$
3	4.5	$3\pi/2$
7	6.8	π
14	13.6	$\pi/2$

Although this analysis and description of the production of O_2^- ions is plausible, it neglects the electron detachment channel and it is obviously an oversimplified description of the reaction dynamics.

At the lowest energies (i.e., $E < 3$ eV), the cross section for the production of O_2^- decreases with decreasing energy. This may be due to the onset of the associative detachment channel (13), which will compete with the various channels for slow-ion production.

Finally, it should be pointed out that the measured charge-transfer cross section is possibly underestimated by as much as 20%, since about 20% of the O_2^- product ions will be collected on element A, if the O_2^- ions have an isotropic angular distribution. Also, similar to N_2 and CO, a small number of negative ions from large-angle elastic or inelastic scattering of the primary ions will undoubtedly reach element B, causing $\sigma_I(E)$ to be overestimated by (in this case) 5–10%.

Figure 9 shows the cross section for electron detachment, $\sigma_e(E)$, for collisions of H^- and D^- with O_2 as a function of relative collision energy. $\sigma_e(E)$, as shown in the figure, is obtained by subtracting 25% of $\sigma_I(E)$ from the measured detachment cross section. This subtraction procedure is important for these systems since the charge-transfer cross section is relatively large by comparison.

Curves representative of the experimental mea-

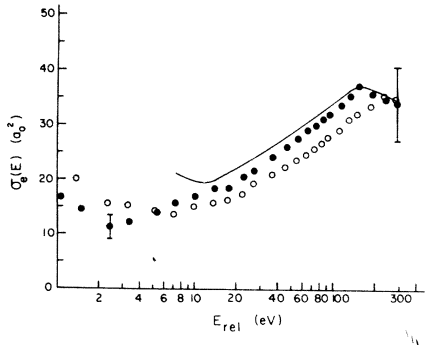

FIG. 9. The total electron detachment cross sections σ_e for H^- and D^- on O_2 are given as a function of relative collision energy. The filled circles correspond to the present results for H^- and the open circles are for D^-. The solid line is a curve representative of the results of Bailey and Mahadevan for electron detachment for collisions of H^- with O_2 and the dotted line is a representative of the results of Risley and Geballe.

surements for $\sigma_e(E)$ by Bailey and Mahadevan[13] and Risley and Geballe,[12] are also given in Fig. 9. It can be seen that the results of Bailey and Mahadevan are in good agreement with the present results. At the highest energies, where the present results overlap with those of Risley and Geballe, the measurements of Risley and Geballe lie about 35% higher than the present results.

For H^-+O_2, there are several mechanisms in addition to direct detachment which can result in the production of free electrons. The charge exchange reaction (14) is endothermic by 0.31 eV for the formation of O_2^- ($v'=0$). However, O_2^- may be produced in a vibrationally stable (i.e., $v' \leq 3$) or unstable (i.e., $v' > 3$) state. For $v' > 3$, O_2^- will autodetach to give free electrons and the neutral O_2 molecule. These electrons will then contribute to the observed detachment cross sections. It is impossible to give a quantitative estimate of the cross section for free-electron production from such a process since there is no way to distinguish these electrons from those produced from direct detachment.

Previous experimental studies have demonstrated that, for selected reactants, associative detachment may compete with direct collisional detachment and charge transfer at very low collision energies.[16,17] Thus, associative detachment [Eq. (13)] may be an important source of detached electrons. The apparent increase in the measured detachment cross section $\sigma_e(E)$ as the energy is decreased below 2.4 eV is probably due to the onset of associative detachment. In this energy region, $\sigma_I(E)$ decreases while $\sigma_e(E)$ increases as the energy is decreased. Finally, the decrease in $\sigma_e(E)$ as E is increased above 150 eV is in accordance with the observations of Risley and Geballe and Bailey and Mahadevan.

D. $H^-(D^-)+CO_2$

The various possible channels of interest for these systems are

$$H^-+CO_2 \rightarrow H+CO_2+e \quad (0.75 \text{ eV}), \tag{19}$$

$$\rightarrow HCO+O^- \quad (\sim 3.6 \text{ eV}), \tag{20}$$

$$\rightarrow CO+OH^- \quad (-0.026 \text{ eV}), \tag{21}$$

$$\rightarrow H+(CO_2^-)^* \rightarrow O^-+CO+H \quad (4.74 \text{ eV}). \tag{22}$$

The energy defects for the ground-state reactants and products are listed for each channel. Figure 10 shows the experimental results for $\sigma_I(E)$ for collisions of H^- and D^- with CO_2 as a function of relative collision energy. These cross sections show distinct peaks at 13 eV with the most pronounced peak being observed for the H^- projectile. In order

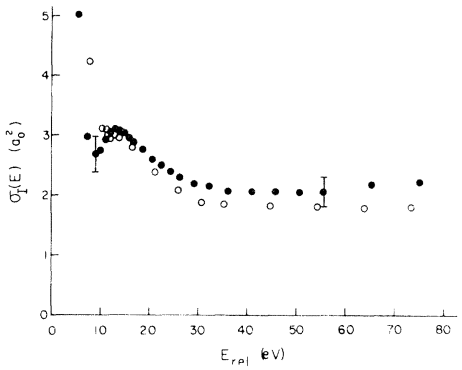

FIG. 10. Total cross sections $\sigma_I(E)$ for collisions of H^- and D^- with CO_2 are given as a function of relative collision energy. The filled circles are the results for H^- and the open circles are for D^-.

to identify the product ions that contribute to $\sigma_I(E)$, experiments were performed for the D^-+CO_2 system with the same differential apparatus as was used for O_2^- identification which was discussed for the H^-+O_2 system. A thorough search was made for O^-, OD^-, O_2^-, and C^- and it was found that at 13 and 17 eV, essentially all of the low-energy product ions were O^-, implying that the peak observed at 13 eV is due to the production of O^- ions. For $E=7.4$ eV, around 85% of the signal was found to be O^- and 15% of the observed ions were OD^-.

Several of the resonance states of CO_2^- (at 4.4, 8.2, and 13.0 eV) are known[18,19] to be instrumental in the production of O^- ions in collisions of electrons with CO_2,

$$e+CO_2 \rightarrow (CO_2^-)^* \rightarrow CO+O^- . \tag{23}$$

It may well be that these same resonances are involved in the production of O^- (Eq. 22) which is observed in these experiments. However, the present total-cross-section measurements cannot establish which, if any, of these resonance states might be involved. It is of interest to point out that doubly differential cross-section measurements for the H^-+CO_2 system performed in this laboratory indicate that these resonances are involved in the inelastic (but nondetaching) scattering of H^- by CO_2. This observation is similar to that reported earlier for the system Cl^-+CO_2.[20]

At the lowest collision energies, $E \lesssim 10$ eV, the partial cross section for large-angle elastic and inelastic scattering for H^- becomes large, rendering an unambiguous interpretation of the low-energy data for $\sigma_I(E)$ impossible.

The results of electron detachment cross sections $\sigma_e(E)$ for collisions of H^- and D^- with CO_2 are presented in Fig. 11 as a function of relative collision energy. The detachment cross sections for both isotopes scale very well with relative collision

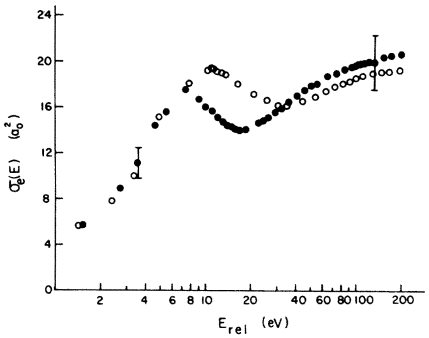

FIG. 11. Absolute total electron detachment cross sections σ_e for H^- and D^- incident on CO_2 are given as a function of relative collision energy. The filled circles are the results for H^- and the open circles are for D^-.

energy in the low-energy (i.e., $E<7$ eV) region. For $7<E<30$ eV, a strong isotope effect (25—30%) is observed where the D^- projectile gives the larger detachment cross section. This isotope effect changes character as the collision energy is increased above 30 eV, where the H^- projectile give the larger detachment cross section. An interesting feature of $\sigma_e(E)$ is that it decreases in a region where $\sigma_I(E)$ increases. The maxima in $\sigma_I(E,H^-)$ observed at $E\simeq 13$ eV may be correlated to the minima in $\sigma_e(E,H^-)$ at the same energy due to a competition among the channels responsible for O^- production and electron detachment.

Another interesting feature of $\sigma_e(E)$ is seen in Fig. 12 where the cross sections are plotted as a function of relative collision velocity. Here the basic features of $\sigma_e(E)$ are seen to scale rather well with velocity, except for the lowest collision velocities where the results scale with energy, as mentioned earlier.

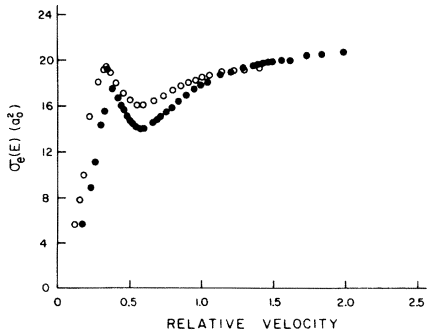

FIG. 12. Absolute total electron detachment cross sections σ_e for H^- and D^- incident on CO_2 are given as a function of relative collision velocity, which is expressed in units of 10^7 cm/sec. The filled circles correspond to the results of H^- and the open circles are for D^-.

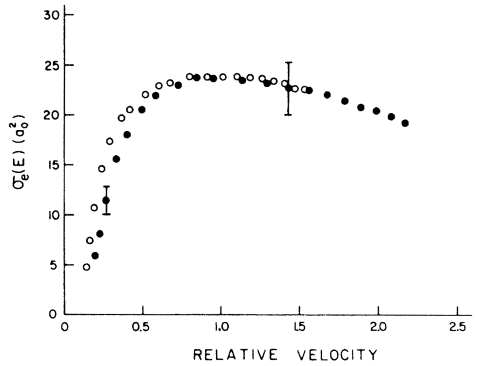

FIG. 13. Absolute total cross sections for electron detachment, σ_e, for H^- and D^- on CH_4 are given as a function of relative collision velocity, which is expressed in units of 10^7 cm/sec. The filled circles are the results for H^- and the open circles are for D^-.

E. $H^-(D^-)+CH_4$

Total electron detachment cross sections $\sigma_e(E)$ for H^- and D^- incident on methane are given in Fig. 13 as a function of relative collision velocity. The cross sections display behavior similar to that which has been observed for other molecular targets: at low collision energies, $\sigma_e(E)$ scales well with relative energy, and at high collision energies the cross sections scale remarkably well with relative collision velocity. One distinctive feature for these reactants is that $\sigma_e(E)$ decreases with increasing collision energy for $E\gtrsim 50$ eV.

Figure 14 shows the cross sections for $\sigma_B(E)$, for collisions of H^- and D^- with methane as a function of relative collision energy. A significant isotope effect is observed for $E\gtrsim 40$ eV, with $\sigma_B(H_2)/\sigma_B(D_2)\sim 2$ for $E=200$ eV. The general shapes of $\sigma_B(E)$ for both isotopes are observed to be similar over the entire energy range.

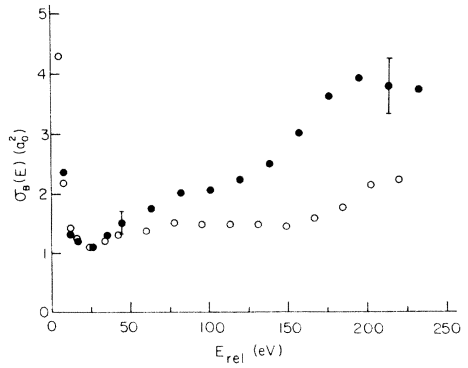

FIG. 14. Total cross sections $\sigma_B(E)$ for collisions of H^- and D^- with CH_4 are given as a function of relative collision energy. The filled circles are the results for H^- and the open circles are for D^-.

It is not known which product ions contribute to $\sigma_B(E)$. The formation of CH_2^- or CH^- is endothermic by a few eV and they may be formed by some direct ion-molecule interaction or by charge transfer to a resonance state of CH_4^-.[21]

A comparison of Fig. 14 with Fig. 13 reveals that $\sigma_B(E)$ increases in a region where $\sigma_e(E)$ decreases. Furthermore, it can be seen that for a particular isotope, the decrease in $\sigma_e(E)$ is comparable with the increase in $\sigma_B(E)$. The process responsible for the structure observed in $\sigma_B(E)$ may then compete with the detachment channel thereby depleting $\sigma_e(E)$ at higher collision energies.

IV. SUMMARY

Measurements of total cross sections for the production of electrons and slow negative ions which result from collisions of H^- and D^- with the molecules N_2, CO, O_2, CO_2, and CH_4 have been made in the energy range extending from a few eV up to several hundred eV. The detachment cross sections for all the molecular targets show similar behavior: at low collision energies, the detachment cross sections scale with relative collision energy, whereas at high collision energies the cross sections scale with relative collision velocity with respect to isotopic substitution.

For the O_2 and CO_2 targets, the detachment cross sections display structure, which in the case of O_2 is attributed to competition between associative detachment and charge transfer. In the case of the CO_2 target a strong isotope effect is observed in the detachment cross section $\sigma_e(E)$, and the structure observed in $\sigma_e(E)$ is attributed to possible competition between direct detachment and charge transfer to the negative-ion resonance states of CO_2^-.

The cross sections for the production of slow negative ions, $\sigma_I(E)$, which is zero for N_2, is found to be negligible for CO. For O_2, the cross section for O_2^- formation is observed to exceed that found for electron detachment. The striking feature of these charge-transfer cross sections is that large oscillations in these cross sections are observed to scale remarkably well with the relative collision velocity. A simple two-state model is used to describe the observed charge transfer. For CO_2 and CH_4, $\sigma_I(E)$ is quite small and displays some structure. In the case of CO_2, the product ions are identified as O^- and it is suggested that the negative-ion states of $(CO_2^-)^*$ may be instrumental in the production of these O^- ions.

ACKNOWLEDGMENTS

The authors are indebted to John Delos and E. A. Remler for helpful conversations concerning several points addressed in this work. This work was supported in part by the Office of Basic Energy Sciences, Division of Chemical Sciences, U.S. Department of Energy.

[1]See, for example, V. Esaulov, D. Dhuicq, and J. P. Gauyacq, J. Phys. B 11, 1049 (1978), and references cited therein for experimental work. For theoretical work, see J. P. Gauyacq, *ibid.* 13, 4417 (1980); R. Taylor and J. B. Delos, Proc. R. Soc. London, Ser. A 379, 179 (1982); 209 (1982), and references cited therein.

[2]J. P. Gauyacq, J. Phys. B 13, L501 (1980).

[3]J. S. Risley, Phys. Rev. A 16, 2346 (1977).

[4]B. K. Annis, S. Datz, R. L. Champion, and L. D. Doverspike, Phys. Rev. Lett. 45, 1554 (1980).

[5]Vu Ngoc Tuan and V. A. Esaulov, J. Phys. B 15, L95 (1982).

[6]M. S. Huq, D. S. Fraedrich, L. D. Doverspike, R. L. Champion, and V. A. Esaulov, J. Chem. Phys. 76, 4952 (1982).

[7]J. L. Mauer and G. J. Schulz, Phys. Rev. A 7, 593 (1973).

[8]J. P. Gauyacq (private communication).

[9]B. T. Smith, W. R. Edwards III, L. D. Doverspike, and R. L. Champion, Phys. Rev. A 18, 945 (1978).

[10]M. S. Huq, L. D. Doverspike, R. L. Champion, and V. A. Esaulov, J. Phys. B 15, 951 (1982).

[11]R. L. Champion, L. D. Doverspike, and S. K. Lam, Phys. Rev. A 13, 617 (1976).

[12]J. S. Risley and R. Geballe, Phys. Rev. A 9, 2485 (1974); J. S. Risley, *ibid.* 10, 731 (1974).

[13]T. L. Bailey and P. Mahadevan, J. Chem. Phys. 52, 179 (1970).

[14]R. L. Champion, L. D. Doverspike, W. G. Rich, and S. M. Bobbio, Phys. Rev. A 2, 2327 (1970).

[15]T. Y. Wu and T. Ohmura, *Quantum Theory of Scattering* (Prentice-Hall, Englewood Cliffs, 1962), p. 234.

[16]A. E. Roche and C. C. Goodyear, J. Phys. B 2, 191 (1969).

[17]J. Comer and G. J. Schulz, Phys. Rev. A 10, 2100 (1974).

[18]C. R. Claydon, G. A. Segal, and H. S. Taylor, J. Chem. Phys. 52, 3387 (1970).

[19]P. J. Chantry, J. Chem. Phys. 57, 3180 (1972).

[20]M. Vedder, L. D. Doverspike, and R. L. Champion, Phys. Rev. A 24, 615 (1981).

[21]P. Marmet and L. Binette, J. Phys. B 11, 3707 (1978).